UNIVERSITAS MUHAMMADIYAH PROF. DR. HAMKA
FAKULTAS FARMASI DAN SAINS
Jl. Limau II, Kebayoran Baru, Jakarta 12130 Tel. (021) 7208177, 722886, Fax. (021) 7261226, 7256620
Islamic Centre, Jl. Delima II/IV, Klender, Jakarta Timur Tlp.: (021) 8611070, Fax. (021) 86603233
Website: www.ffs-uhamka.ac.id; E-mail: ffs@uhamka.ac.id

SURAT TUGAS
MELAKUKAN KEGIATAN PENELITIAN DAN PUBLIKASI
NO. 825/F.03.08/2021

Bismillahirrohmanirrohiim,
Yang bertanda tangan di bawah ini

N a m a	**Dr. apt. Hadi Sunaryo, M.Si.**
NIDN	0325067201
Pangkat /Jabatan Akademik	Penata Muda Tk. I/ Lektor
Jabatan	Dekan
Unit Kerja	Fakultas Farmasi dan Sains UHAMKA Jakarta

Memberikan tugas Penelitian dan Publikasi pada **tahun akademik 2020/2021** kepada:

N a m a	**Dr. apt. Hariyanti, M.Si.**
NID/NIDN	D.03.0606/ 0311097705
Pangkat /Jabatan Akademik	Penata/ III-C
Jabatan Fungsional	LEKTOR
Unit Kerja	Fakultas Farmasi dan Sains UHAMKA Jakarta

Untuk Melaksanakan Penelitian dan Publikasi sebagai berikut:

NO	JUDUL PENELITIAN DAN PUBLIKASI
1.	**"Ligand Based Pharmacophore Modeling, Virtual Screening, and Molecular Docking Studies of Asymmetrical Hexahydro-2H-Indazole Analogs of Curcumin (AIACs) to Discover Novel Estrogen Receptors Alpha (ERα) Inhibitor" pada Indonesian Journal of Chemistry, Tahun 2021**

Demikian surat tugas ini diberikan kepada yang bersangkutan untuk dilaksanakan dengan penuh amanah dan tanggung jawab

Jakarta, 06 Maret 2021
Dekan,

Dr. apt. Hadi Sunaryo, M.Si.

Tembusan Yth:
1. Rektor UHAMKA Jakarta
2. Wakil Rektor I dan II UHAMKA Jakarta
3. Arsip

Ligand Based Pharmacophore Modeling, Virtual Screening, and Molecular Docking Studies of Asymmetrical Hexahydro-2H-Indazole Analogs of Curcumin (AIACs) to Discover Novel Estrogen Receptors Alpha (ERα) Inhibitor

Hariyanti[1], Kusmardi[2], Arry Yanuar[3], and Hayun[3,*]

[1]*Faculty of Pharmacy and Science, Universitas Muhammadiyah Prof. DR. HAMKA, Jl. Delima II/IV, Duren Sawit, East Jakarta 13460, Indonesia*

[2]*Faculty of Medicine, Universitas Indonesia, UI Salemba Campus, Jl. Salemba Raya No. 6, Central Jakarta 10430, Indonesia*

[3]*Faculty of Pharmacy, Universitas Indonesia, Depok 16424, West Java, Indonesia*

* ***Corresponding author:***

email: hayun@farmasi.ui.ac.id

Received: March 8, 2020
Accepted: September 17, 2020

DOI: 10.22146/ijc.54745

Abstract: *The estrogen receptor alpha (ERα) plays an important role in breast development and pro-proliferation signal activation in the normal and cancerous breast. The ERα inhibitors were potentially active as cytotoxic agents against breast cancer. This study was conducted in order to find Asymmetrical Hexahydro-2H-Indazole Analogs of Curcumin (AIACs) as hits of ERα inhibitor. A training set of 17 selected ERα inhibitors was used to create 10 pharmacophore models using LigandScout 4.2. The pharmacophore models were validated using 383 active compounds as positive data and 20674 decoys as negative data obtained from DUD.E. Model 2 was found as the best pharmacophore model and consisted of three types of pharmacophore features, viz. one hydrophobic, one hydrogen bond acceptor, and aromatic interactions. Model 2 was utilized for ligand-based virtual screening 186 of AIACs, AMACs, intermediates, and Mannich base derivative compounds. The hits obtained were further screened using molecular docking, analyzed using drug scan, and tested for its synthesis accessibility. Fourteen compounds were fulfilled as hits in pharmacophore modeling, in which 10 hits were selected by molecular docking, but only seven hits met Lipinski's rule of five and had medium synthesis accessibility. In conclusion, seven compounds were suggested to be potentially active as ERα inhibitors and deserve to be synthesized and further investigated.*

Keywords: *asymmetric hexahydro-2H-indazole analogs of curcumin; AIACs; estrogen receptor alpha inhibitor; ERα inhibitor; pharmacophore modeling; molecular docking; breast cancer*

■ INTRODUCTION

Breast cancer is a disease that occurs almost entirely in women. It is the second leading cause of death by a disease [1]. In 2018, 2.1 million new cases of breast cancer were found. In most countries, this disease was the most commonly diagnosed cancer (154 out of 185) [2]. The estrogen receptor alpha (ERα) plays a role in breast development and the activation of the pro-proliferation signal in normal and cancerous breasts [3]. The growth of breast cancer cells is characterized by the high expression of the receptors [4]. Nowadays, ERα has been developed and tested as molecular targets for the treatment and prevention of breast cancer [5].

Monocarbonyl Analogs of Curcumin (MACs) and Asymmetrical Monocarbonyl Analogs of Curcumin (AMACs) were reported to show better inhibition against cancer cell proliferation of SMMC-7221, MCF-7, and PC-3 compared to curcumin [6]. Diethylamine Mannich base substitution of the phenyl ring of MACs showed increased activity and selectivity of its anticancer properties [7]. Mannich base substitution of AMACs

also showed cytotoxicity potential against HeLa, MCF-7, and WiDr cells [8-9]. The Mannich base acted as an important pharmacophore group in high-potential drugs [10].

Several studies reported that structural modification of symmetrical MACs into symmetrical Hexahydro-2H-Indazole Analog (IAC) exhibited good antioxidant and antitumor activity against Hep G2, WI38, VERO, and MCF-7 cells [11-12]. Some studies also reported that modified compounds with indazole group formation show better anticancer activity [13-14]. However, to the best of our knowledge, there were no reports about the development of AMACs into AIACs and its derivatives. In the present study, we designed 186 structures of AIACs, their derivatives, and intermediate compounds that have different substituents in one of the benzene rings.

In this study, the initial virtual screening of 186 ligand designs was carried out using the Ligand-based virtual screening (LBVS) method. The LBVS methods compare a library of compounds with a known active ligand. Two notable advantages of LBVS methods are that they do not require structural information of a target receptor and that they are faster than structure-based methods [15]. The objective of the study was to discover a new molecular entity of AIACs compounds as hits for ERα inhibitor. The 186 AIACs, AMACs, intermediates, and the Mannich base derivative compounds were screened virtually through ligand-based pharmacophore modeling, structure-based molecular docking, analysis by drug scan, and tested for its synthesis accessibility.

■ COMPUTATIONAL METHODS

Equipment

The hardware used for the calculations, pharmacophore modeling, and molecular docking was a laptop with the following specification: Desktop-AF57S8U, Processor Intel(R) Core(TM) i5-5200 CPU@ 2.20 GHz 2.20 GHz, RAM 16 GB, Operating System Windows 10, 64 bit, Graphic Card AMD Radeon R9-M275 4GB. The software used includes Marvinsketch, LigandScout 4.2, and AutoDockTools (v 4.2) integrated LigandScout software 4.2.

Procedure

Data preparation

The 186 compounds of Asymmetrical Hexahydro-2H-Indazole Analogs of Curcumin (AIACs), AMACs, its intermediate, and Mannich base derivatives were drawn using Marvinsketch (www.chemaxon.com). The structures are shown in Table S1.a–g. A set of data of 34 ERα inhibitor compounds (Table S2.a–b) that consists of four native ligands of ER PDB and 30 other compounds with pIC_{50} values in the range of 4.40 to 9.86, were obtained from www.pubchem.com. The three-dimensional (3D) Estrogen Homo sapiens receptor alpha (ERα) in the complex with E4D600 ligands (PDB code: 1SJ0) was obtained online from a database: NCBI, Research Collaboratory for Structural Bioinformatics Protein Data Bank http://www.pdb.org/pdb/home/ [9,16].

Pharmacophore models preparation and validation

The pharmacophore models were created using LigandScout4.2 [17]. A set of data of 34 ERα inhibitor compounds were grouped according to their cluster of chemical structure similarity. Every cluster of the compounds found was divided in the same proportion randomly to obtain two groups that consist of 17 molecules of ERα inhibitors. Seventeen selected molecules were used as a training set to create ten pharmacophore models. The 383 active compounds and 20674 decoys were used as positive and negative data to validate the pharmacophore models and determine the best pharmacophore model. The validation parameter of the receiver operating characteristic (ROC) that consisted of areas under the curves (AUC 100%) and enrichment factors (EF 1%) was calculated to determine the sensitivity, specificity, and accuracy values. The pharmacophore model with sensitivity > 0.5, specificity > 0.5, AUC value > 0.7, and a hit score > 0.7 was used as a virtual screening model [18].

Ligand-based virtual screening

The virtual screening was used to find AIACs compounds as hits of ERα inhibitors. A database of 186 AIACs and AMACs compounds in .mol file format was put in a screening database of a selected and validated pharmacophore model, then the screening process was

performed until completed. Tamoxifen was used as a positive control. The hit compounds obtained were further sorted based on the best pharmacophore fit values.

Molecular docking study

Docking simulations were carried out to visualize molecular-level interactions between the hits obtained from ligand-based pharmacophore modeling with the active site of ERα (PDB code: 1SJ0) using tamoxifen as a positive control. The docking was done using AutoDock (v4.2) (autodock.scripps.edu/resources/autodock-force field) integrated with LigandScout. The method was validated by extracting the co-crystalline ligand (E4D600) from the ERα crystallographic structure and re-docking the copy of the ligand into its active site. The root-mean-square deviation (RMSD) value of the copy ligand conformation docked at the receptor as compared to the co-crystalline ligand conformation at the same receptor was calculated. The molecular docking was performed by running the Genetic Algorithm parameters 100 times, with algorithm generation number of 27,000, 2,500,000 energy evaluation numbers, and 150 population.

Drug scan and synthesis accessibility analysis

The drug scan and synthesis accessibility were analyzed online on a website (http://swissadme.ch). The analysis involved uploading the ligand file in .smile format. Then, the results were downloaded in excel format.

■ RESULTS AND DISCUSSION

The asymmetrical hexahydro-2H-indazole curcumins (AIACs) were designed as the development of AMACs that refers to the modification of MACs into a symmetrical hexahydro-2H-indazole analog of curcumins (IACs) that provided good results for activity in several cancer cells including breast cancer cells [12]. The AMACs and derivatives exhibited cytotoxicity potential against HeLa, MCF-7, and WiDr cell lines [8-9], thus AIACs were also predicted to have cytotoxic activities as well. The structure of the designed AIACs (Table S1.c–f) had different substituents in one of the benzene rings (–H, –CH_3, –F, –Cl, –OCH_3, –dimethoxy) by considering their different characteristics of electronegativity, electronic charge, and induction effect of the substituents resulting in different geometric shapes for each analog compound. Therefore, the structures had variations in the bonding interactions with the receptors. In the present study, the AIACs were first screened virtually by ligand-based pharmacophore modeling. The hits obtained were then screened by structure-based modeling using molecular docking and further screened again by drug scan and synthesis accessibility analysis to obtain the new bioactive compounds as hits of ERα inhibitor.

Virtual screening (VS) has emerged as a crucial device in identifying bioactive compounds via computational means by employing knowledge on the protein target or known bioactive ligands [19]. Several VS with ERα as a protein target using the structure-based virtual screening (SBVS) protocol had been reported. The protocol screened compounds based on the interactions of the 3D structure of the compounds with the target protein [20-21]. In this study, before the compounds were screened with the SBVS protocol, the compounds were first screened using the LBVS protocol. The compounds were selected based on the similarity of the molecular structure (in terms of shape, pharmacophoric features, molecular fields, etc.), which was believed to show similar behavior. LBVS techniques that consist of substructure mining and fingerprint searches are faster than SBVS techniques (e.g., molecular docking) [22-24]. The benefit of combining docking primarily based digital screening with pharmacophore-primarily based digital screening is that the database of ligands can be pre-filtered by using a pharmacophore query, before assessment using docking simulations. The docking simulations can be published and filtered with the use of a pharmacophore question to dispose of any compounds that fail to bind consistently with the pharmacophore query. The pharmacophore version can in this case be used for the position of the ligand, in addition to the precision of a molecule towards the pharmacophore question; or to guide the placement via a constraint while scoring the extraordinary docking poses [25].

Pharmacophore Model Preparation and Validation

The 3D pharmacophore of the various training sets produced 10 pharmacophore models. The validation of the models by a data set of 383 active compounds as

positive data and 20674 decoys as negative data produced hit scores in the range of 0.7679–0.7718 and three pharmacophore features marked by red, yellow, and purple for HBA, hydrophobic, and AR interaction, respectively. The HBA interaction was formed by the hydroxyl groups in the AR and the ether group; the hydrophobic interaction was formed by the AR, which also showed AR interactions. Fig. 1 presents the 3D pharmacophore model 2 with the type of features and distance between features. The 3D and 2D pharmacophores model of training set E4D600, is shown in Fig. 2, and the types of pharmacophore features marked by color differences in the training set compound are shown in Table 1. The ROC curve of model 2 is shown in Fig. 3. The screening of the ERα inhibitors using model 2 pharmacophore produced the best result in sensitivity = 0.687; specificity = 0.845; AUC 100% = 0.80; accuracy = 0.843; $EF_{1\%}$ = 26.7 and hit score = 0.7712. The set of five hypotheses with sensitivity > 0.5, specificity > 0.5, AUC value > 0.7, and hit score > 0.7 can be used as a virtual screening model [26]. The EF and AUC values showed that the virtual screening method using pharmacophore model 2 was an excellent screening model. The EF and AUC values were worse than the SBVS protocol reported by Yuniarti et al. [27], but it was still better than the results reported by Setiawati et al. [28], and also the EF and AUC values of the SBVS protocol used to identify ligands for ERα in DUD-E (EF = 15.4, AUC = 0.675) [29]. Therefore, the virtual screening of 186 AIACs and AMACs compounds was performed using model 2.

Ligand-Based Virtual Screening

The key features of the pharmacophore interactions of tamoxifen on ERα were hydrophobic interactions, HBAs, and AR interactions (Fig. 1). The virtual screening of 186 AIACs and AMACs compounds resulted in 14 hit compounds that are shown in Table 2. The pharmacophore fit values measured geometric features of molecules for 3D structure-based pharmacophore models. The higher the pharmacophore fit values indicated the higher possibility of the hit to match with the pharmacophore model and show higher activity as ERα inhibitors. The pharmacophore fit values of 14 hits ranged from 45.32 to 53.43. Compounds 3B8,

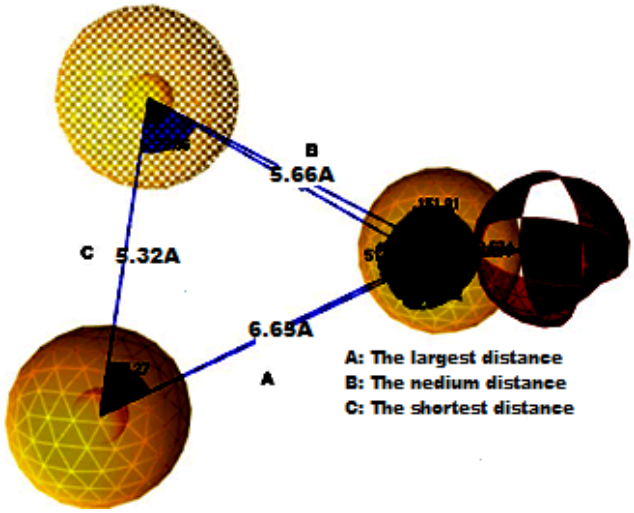

Fig 1. The pharmacophore model 2 features and the distance between features obtained by the LigandScout 4.2 software

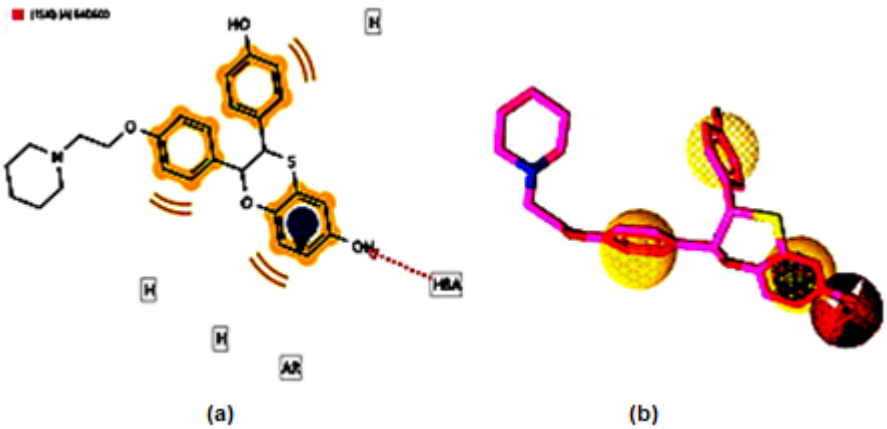

Fig 2. Pharmacophore (a) 2D and (b) 3D models of E4D600 obtained by the LigandScout 4.2 software

Table 1. Types of pharmacophoric features and pharmacophore fit values of 17 training set compounds obtained by the LigandScout 4.2 software. Red, yellow, and purple indicate HBA, hydrophobic, and AR interaction, respectively

No	Active compound name	Type	Matching features*)	Pharmacophore fit
1	4-Hydroxytamoxifen	Training		44.59
2	Arzoxifene	Training		55.22
3	AZD9496	Training		33.87
4	BHPI	Training		43.95
5	Brilanestrant	Training		43.60
6	C3D999	Training		53.99
7	E4D600	Training		54.13
8	Elacestrant	Training		54.11
9	Ferutinin	Training		45.44
10	GW_5638	Training		43.42
11	GW_7604	Training		44.23
12	ICI_164384	Training		44.83
13	Nafoxidine	Training		46.52
14	Raloxifene	Training		55.10
15	Raloxifene_D4	Training		55.14

Table 2. Screening results of 186 AIACS, its intermediate, and derivative compounds with pharmacophore model 2

No	Compound code	Pharmacophore features*)	Pharmacophore fit
1	3B8		53.43
2	3B10		53.39
3	3B7		53.39
4	3A4		46.27
5	3B5		46.22
6	3B2		46.20
7	3B4		45.96
8	3B3		45.95
9	3B1		45.92
10	3A11		45.89
11	3B9		45.79
12	3A12		45.58
13	3B11		45.53
14	3A6		45.32

*) Red, yellow, and purple indicated HBA, hydrophobic, and AR interaction, respectively

3B10, and 3B7 had the best pharmacophore fit values as indicated by their chemical features that are in harmony with the features of the tamoxifen pharmacophore model. None of the hits were Mannich base derivatives. The result was different from the result of *in vitro* evaluation against MCF-7 cell lines of the Mannich base of AMACs reported previously (active but nonselective) [8-9].

Molecular Docking

The structure of ERα in the complex with E4D600 ligands (PDB code: 1SJ0) was selected for in silico study because the parameters were suitable for experimental studies, with a resolution of 1.9 Å, free R-values of 0.272, and working R-values of 0.218. The R-value illustrates a measure of how well the enhanced structure predicts the

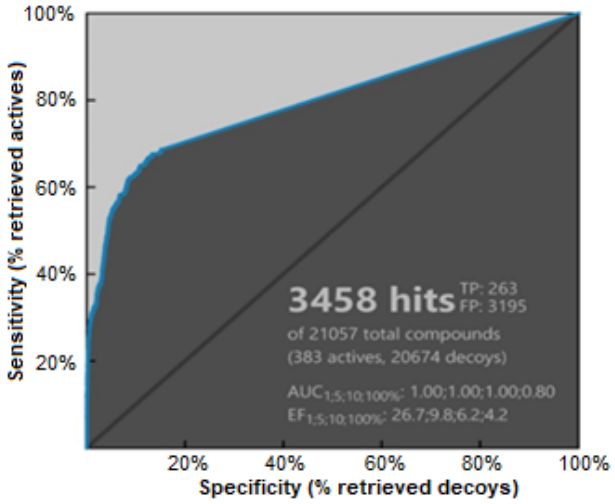

Fig 3. ROC curve model 2

observed data [30]. Interactions between co-crystalline ligand E4D600 with the active site of ERα were dominated by hydrophobic interactions with ARs, and hydrogen bonds with phenoxy and hydroxyl oxygen (Fig. 4 and 5). The best ligand-docking conformation is shown in Fig. 6. The RMSD value of the copy ligand-docking conformation in the active site of ERα compared to the co-crystalline ligand-docking conformation at the same receptor was 0.940 Å (< 2.0 Å), indicating the validity of the protocol.

The results of molecular docking of 14 hit compounds obtained from the ligand-based pharmacophore model are shown in Table 3. The free energy values, ΔG, of the 10 best hits (3A6, 3B1, 3B2, 3B3, 3B4 3B7, 3B8, 3B9, 3B10, and 3B11) did not differ significantly with that of tamoxifen. The interaction of amino acid residues with compounds 3B8 and 3B9 was 14 and 15. It was comparable with the interaction of amino acid with tamoxifen having 17 residues (Table S3 and Table 4). The hydrophobic interaction patterns of compounds 3B7, 3B8, 3B9, 3B10, and 3B11 showed similar triangular patterns and two little differences in the distance (Table S4 and Table 5).

Drug Scan and Synthesis Accessibility Analysis

The drug scan and synthesis accessibility analysis of 10 hit compounds were performed using molecular docking study by running them in www.swissadme.ch. The results showed that seven compounds (3A6, 3B1, 3B2, 3B3, 3B4, 3B7, and 3B11) fulfilled Lipinski's Rule of Five (Table 6) and three compounds (3B8, 3B9, and 3B10) had log P values higher than other ligands (log P > 5), while the synthesis accessibility (SA) values ranged from 4.24 to 4.67. The molecular weights of the ligands were in the range of 334.41–444.95 g/mol which is higher than tamoxifen but still met Lipinski's Rule of Five (MW < 500 g/mol). The rule was a set of in silico guidelines applied to drug discovery to prioritize compounds with a

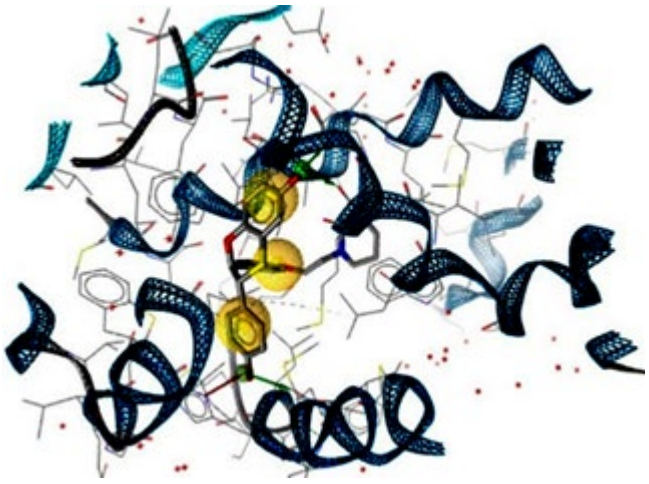

Fig 4. Pharmacophoric features between the native ligand E4D600 with ERα derived from X-ray derivative structures (PDB code: 1SJ0)

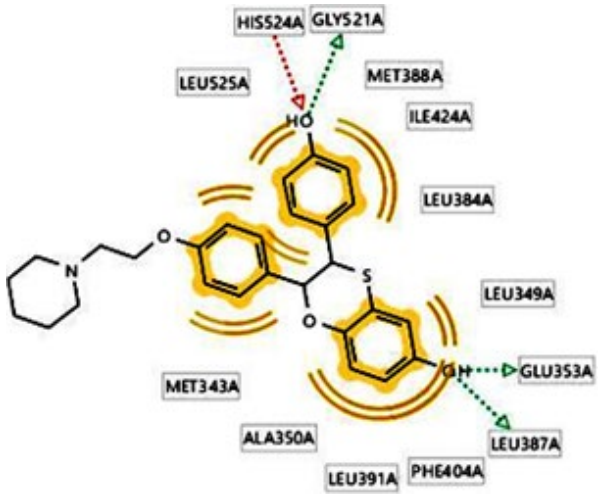

Fig 5. 2D structure visualization describes a hydrophobic bag in the form of a hydrophobic interaction of the native ligand E4D600 with a residue at the receptor. Hydrophobic interactions, donor and acceptor hydrogen bonds are described as yellow balls, green, and red arrows, respectively

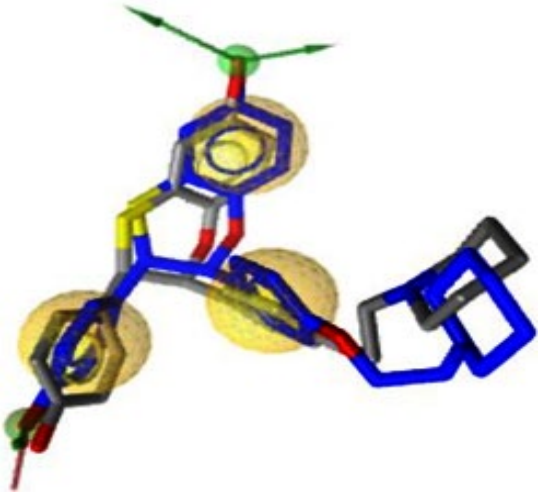

Fig 6. Superpose visualization of co-crystalline ligand (blue) with copy ligand using Autodock 4.2 integrated with Ligandscout 4.2

Table 3. Docking results of design compound molecules with estrogen receptors α (PDB code: 1SJ0)

No	Compound code	ΔG (kcal/mol)
1	3A4	−18.04
2	3A6	−18.11
3	3A11	−14.26
4	3A12	−16.34
5	3B1	−18.36
6	3B2	−18.57
7	3B3	−18.92
8	3B4	−18.37
9	3B5	−16.87
10	3B7	−20.97
11	3B8	−20.88
12	3B9	−20.90
13	3B10	−20.57
14	3B11	−20.47
15	Tamoxifen	−19.87

Table 4. Contact residues of 10 selected compounds and Tamoxifen

Contact residue	Compounds code										
	3A6	3B1	3B2	3B3	3B4	3B7	3B8	3B9	3B10	3B11	Tam*
Leu 525A	√	√	√	√	√	√	√	√	√	√	√
Thr 347A	√	√	√	√	√					√	√
Trp 383A	√	√	√	√	√	√	√	√	√	√	√
Leu 536A			√			√	√	√	√		√
Leu 354A			√			√	√	√	√		√
Ala 350A	√	√	√	√	√	√	√	√	√	√	√
Met 388A	√	√	√			√	√	√	√	√	√
Leu 391A	√			√	√	√	√	√	√	√	√
Phe 404A				√	√		√	√	√	√	√
Leu 428A	√					√	√	√	√	√	√
Leu 384A	√					√	√	√	√	√	√
Ile 424A	√	√	√				√	√	√	√	√
Met 343A	√		√		√		√	√			√
Phe 425A							√	√			√
His 524A	√	√	√								√
Met 421A	√	√	√					√		√	√
Leu 346A		√		√	√		√	√		√	√
Glu 353A				√							
Leu 349A				√	√					√	
Leu 387A				√	√	√			√	√	
Met 522A						√	√	√	√		
Leu 402A							√				

*Tam = Tamoxifen

high probability of absorption [31]. In general, Lipinski's rules describe the solubility of certain compounds that affect the penetration of these compounds across cell membranes through passive diffusion [32]. This rule can

Table 5. The distance between the pharmacophore features of the selected compounds. Distance A, B, and C refer to Fig. 1

No	Compounds code	Distance (Å)		
		A	B	C
1	3B7	6.87	6.26	5.24
2	3B8	6.96	6.21	5.26
3	3B9	6.98	6.86	5.11
4	3B10	6.91	6.22	5.15
5	3B11	6.87	6.28	5.24
Average Distance (Å) ± SD		6.92 ± 0.051	6.37 ± 0.28	5.20 ± 0.066
6	Pharmacophores Features of Model 2	6.65	5.86	5.32
7	Tamoxifen	6.37	5.21	4.91
Difference in average distance of compounds to Model 2		0.27	0.81	0.12
Difference in average distance of compounds to Tamoxifen		0.55	1.16	0.29

Table 6. The prediction results based on Lipinski's rule of five and synthesis accessibility

Compounds code	Prediction using Lipinski's Rule of Five					Synthesis Accessibility
	MW (g/mol)	Log P (Consensus)	Hydrogen Bond Acceptor	Hydrogen bond Donor	TPSA (Å)	
3A6	394.46	3.56	5	2	72.31	4.60
3B1	334.41	3.59	3	2	53.85	4.26
3B2	348.44	3.88	3	2	53.85	4.37
3B3	368.86	4.13	3	2	53.85	4.24
3B4	352.40	3.85	4	2	53.85	4.23
3B7	410.15	4.64	3	1	45.06	4.52
3B8	424.53	5.20	3	1	45.06	4.64
3B9	444.95	5.41	3	1	45.06	4.51
3B10	428.50	5.19	4	1	45.06	4.53
3B11	440.53	4.95	4	1	54.29	4.67
Tamoxifen	371.51	5.77	2	0	12.47	3.01

also be used to predict the pharmacokinetics of a compound as a drug candidate [33].

The SA values of the 10 hits ranged from 4.23 to 4.67, which indicated that the synthesis difficulty was medium and there were no differences among the compounds. However, compounds 3B1, 3B2, 3B3, and 3B4 with SA values in the range of 4.23–4.37 were easier to synthesize than the others. The SA values were based on the analysis of structural fragments of more than 13 million compounds, assuming that the more numerous the molecular fragments, the more difficult the molecules are to prepare. Descriptors correct this fragmental contribution method for molecular size and complexity and the SA values range from 1 (easily synthesized) to 10 (difficult to be synthesized) [34].

■ CONCLUSION

One hundred and eighty-six AIACs, AMACs, intermediates, and their Mannich base derivative compounds were successfully screened using ligand-based pharmacophore modeling, and the hits obtained were further screened using structure-based molecular docking in the active site of ERα, and were analyzed using drug scan and synthesis accessibility. Seven

compounds namely 3A6, 3B1, 3B2, 3B3, 3B4, 3B7, and 3B11 were suggested to be potentially active as ERα inhibitors and deserve to be synthesized and further investigated.

■ SUPPORTING INFORMATION

Table S1.a-g: Structures of the 186 Asymmetrical Hexahydro-2H-Indazole Analogs of Curcumin (AIACs), AMACs, its intermediate, and Mannich base derivative compounds; **Table S2.a:** Four native ligands of ERα receptor; **Table S2.b.:** Data of 30 ERα inhibitor compounds **Table S3:** 2D and 3D visualization results of 10 selected compounds and Tamoxifen docked at 1SJ0 receptors; **Table S4:** 2D and 3D visualization of chemical features with triangular patterns.

■ ACKNOWLEDGMENTS

This work was supported by the Doctoral Program Dissertation Grant Universitas Indonesia, No.: NKB-0092/UN2.R3.1/HKP.05.00/2019, which was gratefully appreciated.

■ AUTHOR CONTRIBUTIONS

HYT conducted the experiment; HY, AY and KMD supervised the experiment; HYT, HY, and AY wrote and revised the manuscript. All authors agreed to the final version of this manuscript.

■ REFERENCES

[1] Mellatyar, H., Talaei, S., Nejati-Koshki, K., and Akbarzadeh, A., 2016, Targeting HSP90 gene expression with 17-DMAG nanoparticles in breast cancer cells, *Asian Pac. J. Cancer Prev.*, 17 (5), 2453–2457.

[2] Bray, F., Ferlay, J., Soerjomataram, I., Siegel, R.L., Torre, L.A., and Jemal, A., 2018, Global cancer statistics 2018: GLOBOCAN estimates of incidence and mortality worldwide for 36 cancers in 185 countries, *CA Cancer J. Clin.*, 68 (6), 394–424.

[3] Caldon, C.E., 2014, Estrogen signaling and the DNA damage response in hormone dependent breast cancer, *Front. Oncol.*, 4, 1–9.

[4] Hayashi, S.I., Eguchi, H., Tanimoto, K., Yoshida, T., Omoto, Y., Inoue, A., Yoshida, N., and Yamaguchi, Y., 2003, The expression and function of estrogen receptor alpha and beta in human breast cancer and its clinical application, *Endocr. Relat. Cancer*, 10 (2), 193–202.

[5] den Hollander, P., Savage, M.I., and Brown, P.H., 2013, Targeted therapy for breast cancer prevention. *Front. Oncol.*, 3, 250.

[6] Revalde, J.L., Li, Y., Hawkins, B.C., Rosengren, R.J., and Paxton, J.W., 2015, Heterocyclic cyclohexanone monocarbonyl analogs of curcumin can inhibit the activity of ATP-binding cassette transporters in cancer multidrug resistance, *Biochem. Pharmacol.*, 93 (3), 305–317.

[7] Yerdelen, K.O., Gul, H.I., Sakagami, H., and Umemura, N., 2015, Synthesis and biological evaluation of 1, 5-bis (4-hydroxy-3-methoxyphenyl) Penta-1, 4-dien-3-one and its aminomethyl derivatives, *J. Enzyme Inhib. Med. Chem.*, 30 (3), 383–388.

[8] Kurnia, A., Saputri, F.C., and Hayun, H., 2019, Synthesis and anticancer potential of aminomethyl derivatives of methyl-substituted asymmetrical curcumin mono-carbonyl, *J. Appl. Pharm. Sci.*, 9 (8), 18–24.

[9] Prasetyaningrum, P.W., Bahtiar, A., and Hayun, H., 2018, Synthesis and cytotoxicity evaluation of novel asymmetrical mono-carbonyl analogs of curcumin (AMACs) against Vero, HeLa, and MCF7 cell lines, *Sci. Pharm.*, 86, 25.

[10] Bala, S., Sharma, N., Kajal, A., Kamboj, S., and Saini, V., 2014, Mannich bases: An important pharmacophore in present scenario, *Int. J. Med. Chem.*, 2014, 191072.

[11] Bayomi, S.M., El-Kashef, H.A., El-Ashmawy, M.B., Nasr, M.N.A., El-Sherbeny, M.A., Badria, A., Abou-zeid, L.A., Ghaly, M.A., Abdel-Aziz, N.I., 2013, Synthesis and biological evaluation of new curcumin derivatives as antioxidant and antitumor agents, *Med. Chem. Res.*, 22 (3), 1147–1162.

[12] Bayomi, S.M., El-Kashef, H.A., El-Ashmawy, M.B., Nasr, M.N.A., El-Sherbeny, M.A., Abdel-Aziz, N.I., El-Sayed, M.A.A., Suddek, G.M., El-Messery, S.M., and Ghaly, M.A., 2015, Synthesis and biological

evaluation of new curcumin analogues as antioxidant and antitumor agents: Molecular modeling study, *Eur. J. Med. Chem.*, 101, 584–594.

[13] Reddy, M.T., Rddy, V.H., Reddy R.C.K., Reddy, V.K., and Reddy, Y.V.R., 2010, Synthesis and molecular docking studies of new substituted indazole derivatives for anti-breast cancer activity, *Der Pharma Chem.*, 6 (6), 411–417.

[14] Plescia, S., Raffa, D., Plescia, F., Casula, G., Maggio, B., Daidone, G., Raimondi, M.V., Cusimano, M.G., Bombieri, G., and Meneghetti, F., 2010, Synthesis and biological evaluation of new indazole derivatives, *ARKIVOC*, 10, 163–177

[15] Shin, W.H., Zhu, X., Bures, M.G., and Kihara, D., 2015, Three-dimensional compound comparison methods and their application in drug discovery, *Molecules*, 20 (7), 12841–12862.

[16] Li, Q., Chen, J., Luo, S., Xu, J., Huang, Q., and Liu, T., 2015, Synthesis and assessment of the antioxidant and antitumor properties of asymmetric curcumin analogues, *Eur. J. Med. Chem.*, 93, 461–469.

[17] Wolber, G., and Langer, T., 2005, LigandScout: 3-D pharmacophores derived from protein-bound ligands and their use as virtual screening filters, *J. Chem. Inf. Model.*, 45 (1), 160–169.

[18] Seidel, T., Ibis, G., Bendix, F., and Wolber, G., 2010, Strategies for 3D pharmacophore-based virtual screening, *Drug Discovery Today Technol.*, 7 (4), e221–e228.

[19] Kar, S., and Roy, K., 2013, How far can virtual screening take us in drug discovery?, *Expert Opin. Drug Discovery*, 8 (3), 245–261.

[20] Maruthanila, V.L., Elancheran, R., Roy, N.K., Bhattacharya, A., Kunnumakkara, A.B., Kabilan, S., and Kotoky, J., 2019, In silico molecular modelling of selected natural ligands and their binding features with estrogen receptor alpha, *Curr. Comput. Aided Drug Des*., 15 (1), 89–96.

[21] Afreen, S., Uddin, N., Mehjabin, K.Z., Niketa, T.K., Nesa, F., Akther, S.,Akther, S., Chakraborty, S., Chowdhury D., and Akther, N., 2018, *In silico* molecular docking approach of some selected isolated phytochemicals from *Phyllanthus emblic* against breast cancer, *BJSTR*, 10 (2), 7661–7665.

[22] Banegas Luna, A.J., Cerón-Carrasco, J.P., and Pérez-Sánchez, H., 2018, A review of ligand-based virtual screening web tools and screening algorithms in large molecular databases in the age of big data, *Future Med. Chem.*, 10 (22), 2641–2648

[23] Sun, Y., Zhou, H., Zhu, H., and Leung, S.W., 2016, Ligand-based virtual screening and inductive learning for identification of SIRT1 inhibitors in natural products, *Sci. Rep.*, 6 (1), 19312.

[24] Liu, C., Yin, J., Yao, J., Xu, Z., Tao, Y., and Zhang, H., 2020, Pharmacophore-based virtual screening toward the discovery of novel anti-echinococcal compounds, *Front. Cell. Infect. Microbiol.*, 10, 118.

[25] Qing, X., Lee, X.Y., De Raeymaecker, J., Tame, J., Zhang, K., De Maeyer, M., and Voet, A., 2014, Pharmacophore modeling: Advances, limitations, and current utility in drug discovery, *J. Recept. Ligand Channel Res.*, 7, 81–92.

[26] Lone, M.Y., Manhas, A., Athar, M., and Jha, P.C., 2018, Identification of InhA inhibitors: A combination of virtual screening, molecular dynamics simulations, and quantum chemical studies, *J. Biomol. Struct. Dyn.*, 36 (11), 2951–2965.

[27] Yuniarti, N., Mungkasi, S., Yuliani, S.H., and Istyastono, E.P., 2019, Development of a graphical user interface application to identify marginal and potent ligands for estrogen receptor alpha, *Indones. J. Chem.*, 19 (2), 531–537.

[28] Setiawati, A., Riswanto, F.D.O., Yuliani, S.H., and Istyastono, E.P.2014, Retrospective validation of a structure-based virtual screening protocol to identify ligands for estrogen receptor alpha and its application to identify the alpha-mangostin binding pose, *Indones. J. Chem*., 14 (2), 103–108.

[29] Mysinger, M.M., Carchia, M., Irwin, J.J., and Shoichet, B.K., 2012, Directory of useful decoys, enhanced (DUD-E): Better ligands and decoys for better benchmarking, *J. Med. Chem.*, 55 (14), 6582–6594.

[30] Kim, S., Wu, J.Y., Birzin, E.T., Frisch, K., Chan, W., Pai, L.Y., Yang, Y.T., Mosley, R.T., Fitzgerald, P.M.D., Sharma, N., Dahllund, J., Thorsell, A.G.,

DiNinno, F., Rohrer, S.P., Schaeffer, J.M., and Hammond, M.L., 2004, Estrogen receptor ligands. II. Discovery of benzoxathiins as potent, selective estrogen receptor alpha modulators, *J. Med. Chem.*, 47 (9), 2171–2175.

[31] Doak, B.C., Over, B., Giordanetto, F., and Kihlberg, J., 2014, Oral druggable space beyond the rule of 5: Insights from drugs and clinical candidates, *Chem. Biol.*, 21 (9), 1115–1142.

[32] Lipinski, C.A., Lombardo, F., Dominy, B.W., and Feeney, P.J., 1997, Experimental and computational approaches to estimate solubility and permeability in drug discovery and development settings, *Adv. Drug Delivery Rev.*, 23 (1-3), 3–25.

[33] Benet, L.Z., Hosey, C.M., Ursu, O., and Oprea, T.I., 2016, BDDCS, the rule of 5 and drugability, *Adv. Drug Delivery Rev.*, 101, 89–98.

[34] Daina, A., Michielin, O., and Zoete, V., 2017, SwissADME: A free web tool to evaluate pharmacokinetics, drug-likeness and medicinal chemistry friendliness of small molecules, *Sci. Rep.*, 7, 42717.

UNIVERSITAS MUHAMMADIYAH PROF. DR. HAMKA
FAKULTAS FARMASI DAN SAINS
Jl. Limau II, Kebayoran Baru, Jakarta 12130 Tel. (021) 7208177, 722886, Fax. (021) 7261226, 7256620
Islamic Centre, Jl. Delima II/IV, Klender, Jakarta Timur Tlp.: (021) 8611070, Fax. (021) 86603233
Website: www.ffs-uhamka.ac.id; E-mail: ffs@uhamka.ac.id

SURAT TUGAS
MELAKUKAN KEGIATAN PENELITIAN DAN PUBLIKASI
NO. 702/F.03.08/2021

Bismillahirrohmanirrohiim,
Yang bertanda tangan di bawah ini

N a m a	**Dr. apt. Hadi Sunaryo, M.Si.**
NIDN	0325067201
Pangkat /Jabatan Akademik	Penata Tk. I, IIId/ Lektor Kepala
Jabatan	Dekan
Unit Kerja	Fakultas Farmasi dan Sains UHAMKA Jakarta

Memberikan tugas Penelitian dan Publikasi pada **tahun akademik 2021/2022** kepada:

N a m a	**Dr. apt. Hariyanti, M.Si.**
NID/NIDN	D.03.0606/ 0311097705
Pangkat /Jabatan Akademik	Penata/ III-C
Jabatan Fungsional	LEKTOR
Unit Kerja	Fakultas Farmasi dan Sains UHAMKA Jakarta

Untuk Melaksanakan Penelitian dan Publikasi sebagai berikut:

NO	JUDUL PENELITIAN DAN PUBLIKASI
1.	**"Identification of amylase activity from vannamei shrimps' (Litopenaeus vannamei) digestive tract using size exclusion chromatography method" di Jurnal Natural Tahun: 2021.**

Demikian surat tugas ini diberikan kepada yang bersangkutan untuk dilaksanakan dengan penuh amanah dan tanggung jawab

Jakarta, 05 September 2021
Dekan,

Dr. apt. Hadi Sunaryo, M.Si.

Tembusan Yth:
1. Rektor UHAMKA Jakarta
2. Wakil Rektor I dan II UHAMKA Jakarta
3. Arsip

Jurnal Natural
Vol. 21, (3) 2021
DOI 10.24815/jn.v21i3.18874
pISSN 1411-8513
eISSN 2541-4062

ORIGINAL RESEARCH

Identification of amylase activity from vannamei shrimps' (*Litopenaeus vannamei*) digestive tract using size exclusion chromatography method

HARIYANTI[1], RENA NADIA PERMATA ASRY[1], HANIFAH RAHMI[1]*

[1]Faculty of Pharmacy and Science, Universitas Muhammadiyah Prof. Dr. HAMKA, DKI Jakarta, Indonesia

Abstract. Vannamei shrimps (*Litopenaeus vannamei*), also known as white leg shrimps are widely cultivated and consumed by many people. However, most consumers have removed the shrimp's head which integrates with its digestive tract. The digestive tract of white leg shrimp contains digestive enzymes, including amylase. This study aimed to determine the protein content and amylase activity from Vannamei shrimps' digestive tract using the size exclusion chromatography method. The protein isolation of size exclusion chromatography was prepared in three steps, namely; centrifugation, precipitation, and dialysis. The protein from the dialysis step was purified by using gel filtration chromatography. Each obtained fraction was determined the protein content and amylase activity by using spectrophotometer UV-Vis method. The results showed that the fraction of 108th had the highest protein content and amylase activity with a value of 0.85 mg/ml and 25.66U/ml respectively.

Keywords: amylase activity, *Litopenaeus vannamei*, protein content, size exclusion chromatography

INTRODUCTION

Vannamei shrimp is one of the fisheries commodities that have high economic value in domestic and global markets, and its production is also increasing every year. Therefore, there are a lot of wastes produced from shrimps and most of them are from the head and shell wastes. The head of shrimp contains the whole digestive tract with digestive enzymes, including amylase, lipase, and protease.

Amylase is classified as saccharides (an enzyme that cuts polysaccharides). Amylase is a digestive enzyme, mainly carried out by the pancreas and salivary glands (1). Amylase enzymes have many essential roles in the food, detergent, textile, paper, and bioethanol industries. In the pharmaceuticals field, amylase is used as a raw material for drug digestion disorders.

The use of amylase as a result of isolation is considered ineffective because its enzyme activity is still low, so the size exclusion chromatography is a method that can be used to increase the activity of the enzyme. The separation and purification of the enzyme are necessary to increase the enzyme activity and obtain optimal and efficient catalysts (2). Enzyme separation was carried out to obtain protein fraction of the Vannamei shrimps' (*Litopenaeus vannamei*) digestive tract which had the highest amylase enzyme activity.

The process of enzyme separation was carried out through precipitation and gel filtration chromatography method, while precipitation is carried out by using ammonium sulfate. Ammonium sulfate is used because it has several benefits, such as it has high solubility, it does not affect the enzymes activity, it has sufficient deposition power, it has a stabilizing effect on most enzymes, and also it can be used at various pH and low prices (3).

Gel filtration chromatography is a method of separating proteins based on a protein molecular size by passing it into a column containing expanded gel particles (4). The principle of gel filtration chromatography process is similar to the column chromatography, but it differs only in the stationary phase used, where the gel filtration chromatography uses by the researcher is Sephadex G-100 as stationary phase.

The previous study revealed that gel filtration chromatography was able to separate amylase enzyme from the digestion of Vannamei shrimp was 2.97 ± 0.11 units/mL (5). Other studies showed that amylase activity isolated from

*Corresponding Author:
hanifah_rahmi@uhamka.ac.id

Received: December 2020| Revised: September 2021 | Accepted: September 2021

shrimp with several probiotic Bioremediation-Bacillus sp was 60.3 ± 3.8 units/ml (6). Anhar (2018) reported that 80% of ammonium sulfate was able to precipitate amylase enzyme 30.52 U/ml (7). This study aimed to isolate and determine amylase from Vannamei shrimps' (*Litopenaeus vannamei*) digestive tract by using gel filtration chromatography method.

METHODOLOGY

Extraction and Precipitation Stages

Researcher used as much as 540 g sample of the digestive tract from the shrimp head then mashed with a grinder machine, while it was adding drop by drop of cold phosphate buffer pH 7. After that, the mixture was centrifuged (Thermo Scientific) at a cold temperature of 10,000 rpm for 15 minutes. The supernatant that was obtained was added drop wise an ammonium sulfate solution under constant stirring to precipitate the enzyme. The precipitation was centrifuged again at 10.000 rpm 4ºC for 15 minutes in cold temperature. The obtaining residue is used for dialysis.

Dialysis

The cellophane tube bag was filled with a deposit resulted from the deposition process which it would be dialyzed, and the other tip was bound again. The result of precipitation was deposited into cellophane with a size of 14 kDa and then it was also dialyzed by immersing cellophane with a pH 7 buffer solutions. Dialysis was carried out by using a magnetic stirrer at 125 rpm, at 4°C for 7x24 hours with solvent replacement every 3 hours. If there were not any dialysis deposits have been formed from this stage (8), the researcher would mix the phosphate buffer solution pH 7 with $BaCl_2$ and HCl (1: 1).

Determination of Protein

Determination of protein content began by creating two parts, namely blank and test. Pipette with 0.1 ml of enzyme and added it with 5 ml of Bradford were used in the test, while for the blank, it contained 0.1 ml of distilled water and 5 ml of Bradford reagent. Then, the test and blank were incubated with a water bath at 37 ºC for 10 minutes. After incubation, the test and blank would be measured at a wavelength of 595 nm (9).

Size Exclusion Chromatography

Sephadex was developed by using phosphate buffer. As much as 1.9 ml of the enzyme fraction with the highest specific activity value was obtained from the deposition of ammonium sulfate it put into a column with a Sephadex G-100 matrix (column length of 20.5 cm and diameter of 2.4 cm) which was balanced with phosphate buffer and the elution rate was regulated. The sample was eluted with a similar phosphate buffer (10). The volume of each fraction collected was 1.5 ml and each fraction absorbed was measured by the researcher, then the enzyme activity test was carried out.

Amylase Activity

As much as 0.1 ml of Amylum 1% was added into the crude extract, then it incubated at 37ºC for 5 minutes. Enzyme activity was stopped by adding 2 ml of DNS, incubated at 37ºC for 5 minutes. Amylase activity was determined by using a spectrophotometer at a wavelength of 540 nm (11).

Data Analysis

Amylase activity:

$$\frac{M\ Glucose\ \left(\frac{\mu g}{ml}\right)\ x\ 1000\ x\ fp}{Mr\ Glucose\ x\ Incubation\ time} \quad \text{..... (1)}$$

From the formula above, it can be explained as M Glucose is the glucose produced from starch hydrolysis, fp is the dilution factor, and Mr Glucose is the relative molecules of glucose.

RESULTS AND DISCUSSION

Extraction and Precipitation

Vannamei shrimps were determined in the Zoology section of the Indonesian Institute of Sciences' Biology Research Center (LIPI) Cibinong. The results of these determinations indicated that the sample was indeed Vannamei shrimp. The determination of the sample aimed to find out the truth of the sample used. Determination was conducted in the next stage so that there was no error in the preparation of the sample that was used in the research.

Enzymes were one of the materials that could be used for health, food, and industry needs. This study used a protein that was obtained from the digestive tract of shrimps. The digestive tract in Vannamei shrimps' head could be a source of enzymes (12). The result of sample obtained 540.0985 g a digestive tract.

Enzyme extraction separated one or more components in a mixture using a solvent with the polarity principle. The polarity principle in extraction applied PBS (phosphate buffer saline) pH 7. Isolation was conducted because the enzyme was in the cells of the shrimp's digestive tract. Therefore, the extraction process was conducted by destroying the

digestive tract of shrimp (13). Vannamei shrimp gastrointestinal enzyme extraction results could be seen in (Table 1).

Table 1. Results of Vannamei shrimps digestion enzyme extraction.

No.	Information	Result
1.	Vannamei Shrimps Samples	7.11 kg
2.	Vannamei Shrimps Digestion	540.0985 g
3.	Enzyme extract	1080 ml
4.	Supernatant	968 ml
5.	Precipitate	30 ml
6.	% Yield Vannamei	7.5963%
7.	Shrimps Digestion % Yield Sediment	5.5545%

Based on the table above, the shrimp's digestive tract obtained was 540.0985 g from 7.11 kg of Vannamei shrimp. Vannamei Shrimps' digestive tract obtained a yield of 7.5963%. These results achieved a higher result when compared with Anhar's result (7). In Anhar research (2018), it had a Vannamei shrimp digestive tract of 520.39 g and a digestive tract yield of 4.3365% (7). The factor that caused the difference was the weight of the shrimp used in this study was heavier by 20 g so that the yield and the number of shrimp digestive tract samples obtained were also higher.

Enzyme precipitation was carried out with the aim of the protein deposition and the protein was precipitated to separate it from other molecules besides protein. Enzyme precipitation used in this research was 70% ammonium sulfate. According to Purwanto (2016) stated that higher levels of ammonium sulfate would precipitate a more hydrophilic protein. Therefore, the protein deposited in this process showed that many crude enzyme extracts had proteins with high hydrophilic properties (3).

The crude enzyme extract obtained as much as 1080 ml and then it was centrifuged. The first centrifugation was done to separate proteins and cell debris. Cells that were not expected were still mixed with proteins, so they might be separated from proteins. The second centrifugation process produced a precipitate of 30 ml. 30 ml of pellet contained a lot of protein because it was deposited due to the salting-out process. The withdrawal of water would be taken by salt so that the binding of protein with water became weak and the bond between protein and protein so that the protein became precipitated (3). The deposition of protein caused a high salt level in the sample, so it needed to be separated through a dialysis process.

Dialysis

The purpose of the dialysis process was to remove excess salts from the precipitation, and then the low molecular protein came out of the sample through the cellophane membrane. Ammonium sulfate salt could be removed by the process of dialysis using cellophane membranes (14). The cellophane membrane had a size of 14 kDa. Therefore, the cellophane membrane could hold molecules larger than 14 kDa.

Size Exclusion Chromatography

Gel filtration chromatography was one of the methods used for enzyme separation. Large molecules would pass through the pore of the Sephadex first and smaller particles would go down longer because they were stuck in the pore. Spectrophotometer readings were performed at a wavelength of 280 nm. A wavelength of 280 nm was used to determine whether there was a protein concentration in it. Therefore, it was necessary to test the activity to get more specific results.

The results obtained from filtrate gel filtration chromatography were 139 fractions. Based on Figure 1 of the 139 fractions obtained, 14 fractions with absorbance above 0.15 were separated and carried out enzyme activity tests. The reason was that the 14 fractions were considered to have more amylase enzymes compared to other fractions.

The amylase enzyme obtained was expected to have the highest amylolytic activity in breaking down starch into glucose. The results obtained from the dialysis process were in the form of dialysate. The dialysate was obtained in 20 ml. The dialysate contained an enzyme extract that did not contain ammonium sulfate and low molecular protein. The final result of dialysis was identified by using the sulfate test. It was characterized by the absence of white deposits.

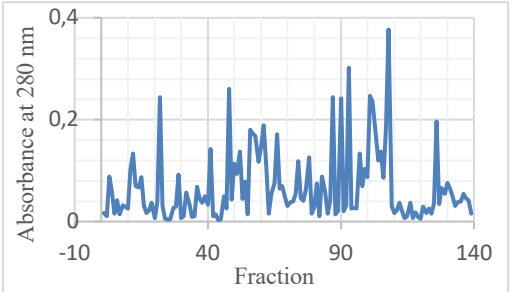

Figure 1. Chromatogram of protein absorption at 280 nm.

Amylase Activity

Amylase enzyme activity values were obtained through calculations integrated into the linear regression formula y = 0.0534 + 0.02165x. The value of y in the regression equation was the difference between the absorbance of blanks and tests, while the x value was obtained from the glucose level collected. The r-value in this study was 0.9968. r-value was expressed as close to 1, and it could be concluded that the correlation coefficient was feasible, which means the points on the calibration curve were close to the slope.

Total enzyme activity was calculated in U (units) per ml of enzyme extract. One unit of an enzyme (U) was defined as the number of ml of the catalyst needed to produce 1 µmol substrate every minute. This showed that the amylase enzyme in the 108th fraction had the highest amylolytic activity in converting starch to glucose. The highest activity of amylase, which was obtained in the 108th fraction with an activity of 25.66 U/mL (Table 2).

Table 2. Amylase activity of selected fraction.

Fraction	Enzyme Activity Total (U/mL)	Fraction	Enzyme Activity Total (U/mL)
22	15.44	87	14.09
48	17.27	90	12.43
56	3.00	93	19.82
57	3.26	101	2.58
58	1.95	102	15.27
61	7.56	**108**	**25.66**
66	5.29	126	2.43

The results of the protein level test from the Vannamei shrimp digestive tract could be seen in Table 3. The protein concentration was determined by Bradford method. Based on Table 3, protein levels were concentrated of 0.1215 mg/ml (before dialysis process), 0.1181 mg/ml (dialysate), and 0.0852 mg/ml (108th chromatography fraction). The results showed the highest protein content in the sample before the dialysis process. The samples before dialysis contain a lot of protein, it caused by the absence of a separation process. Then, there was a decrease in protein content, especially dialysate, because of the protein precipitation with 70% ammonium sulfate salt. That was not all protein separated from the extracted sample so that the protein content after dialysis got lower yields compared with before dialysis. The reduction of protein level in the 108th fraction was also caused by dilution that occurs during the chromatography process.

Table 3. Protein concentration at each stage of separation.

Stages	Protein (mg/mL)	Amylase Activity Total (U/mL)	Specific Activity (U/mg)
Salting-Out	0.1215	17.08	140.51
Dialysis	0.1181	19.96	169.01
108th chromatography fraction	0.0852	25.66	301.17

The data of amylase and protein on the white shrimp's digestive tract in the current study indicated an increase in enzyme activity and a decrease in protein levels along with the level of purity. The enzyme activity was concerning to the total protein present (i.e., the specific activity) could be determined and used as a measure of enzyme purity. It was clear that the higher the level of purification, the greater the cost of enzyme activity (15). Anhar (2018) reported that the protein concentration and the amylase activity from salting-out precipitation of 12 kg white shrimps, respectively, about 0.117 mg/mL and 30.52 U/mL. Our current research might be explained by different amounts of white shrimp and ammonium sulfate percentage, affecting different protein levels and activities. In addition, dilution factors and the absence of protease inhibitors, like PMSF, could influence the decrease in enzyme content.

CONCLUSION

In summary, the highest activity from size exclusion chromatography (SEC) was obtained at the 108th fraction with an amylase activity of 25.6571 U/mL and specific activity was 30.10 U/mg. This value showed that the protein fraction of Vannamei shrimp digestion had amylase activity, even though it was not high enough. Further investigations on SEC conditions, such as pH, temperature, retention factor, and gel matrix type, were considered to find maximum enzyme activity.

ACKNOWLEDGMENT

This research was supported by Universitas Muhammadiyah Prof DR. HAMKA of Research Institution, which was gratefully appreciated.

REFERENCE

[1] Bonnefond, A.; Yengo, L.; Dechaume, A.; Canouil, M.; Castelain, M.; Roger, E.; Allegaert, F.; Caiazzo, R.; Raverdy, V.; Pigeyre, M.; Arredouani, A.; Borys, J.M.; Marchal, C.L.; Weill, J.; Roussel, R.; Balkau, B.; Marre, M.; Pattou, F.; Brousseau, T.; Froguel, P. 2017. Relationship between salivary/pancreatic amylase and body mass index: A systems biology approach. *BMC Med*. **15(1)** 1–10.

[2] Wingfield, P.T. 2015. Overview of the purification of recombinant proteins. *Curr Protoc Protein Sci*. **80(1)** 61.1-61.35.

[3] Purwanto, M.G.M. 2016. The Role and Efficiency of Ammonium Sulphate Precipitation in Purification Process of Papain Crude Extract. *Procedia Chem*. **18** 127–31.

[4] Bouvier, E.S.P.; Koza, S.M. 2014. Trends in analytical chemistry advances in size-exclusion separations of proteins and polymers by UHPLC. *Trends Anal Chem*. **63** 85–94. Available from: http://dx.doi.org/10.1016/j.trac.2014.08.002

[5] Lestari, D.P. 2018. Aktivitas Enzim Pencernaan Udang Vaname (Penaeus vannamei) yang Diberikan Pakan Berbahan Baku Tepung Skeletonema costatum. *J Perikanan*. **8(1)** 71–75. Available from: https://jperairan.unram.ac.id/index.php/JP/article/view/79/78

[6] Aslamyah, S. 2011. Kualitas Lingkungan dan Aktivitas Enzim Pencernaan Udang Vannamei (Litopenaeus vannamei) Pada Berbagai Konsentrasi Probiotik Bioremediasi-Bacillus sp. *Fish Sci*. **1(2)** 161–78. Available from: https://ppjp.ulm.ac.id/journal/index.php/fs/article/view/6709

[7] Anhar, D. 2018. Analisis SDS-Page Enzim Pencernaan pada Fraksi Ammonium Sulfat 80% dari Saluran Pencernaan Udang Vannamei (Litopenaeus vannamei). *Skripsi*. Jakarta: Universitas Muhammadiyah Prof. DR. HAMKA.

[8] Mayasari. 2016. Pemurnian Enzim Amilase Kasar dari Bakteri Amilolitik Endogenous Bekatul Secara Parsial Menggunakan Ammonium Sulphate. *Skripsi*. Malang: Universitas Islam Negeri Maulana Malik Ibrahim.

[9] Malle, D.; Telussa, I.; Lasamahu, A.A. 2015. Isolation and Characterization of Papain from The Latex of Papaya (Carica papaya L). *Ind J Chem Res*. **2** 182–189. Available from: https://ojs3.unpatti.ac.id/index.php/ijcr/article/view/94

[10] Hong, P.; Koza, S.; Bouvier, E. 2012. Size-Exclusion Chromatography for The Analysis of Protein Biotherapeutics and Their Aggregates. *J Liq Chromatogr Relat Technol*. **35(20)** 2923–2950. Available from: https://www.ncbi.nlm.nih.gov/pubmed/23378719

[11] Supriyatna, A.; Amalia, D.; Jauhari, A.A.; Holydaziah, D. 2015. Aktivitas Enzim Amilase, Lipase, dan Protease dari Larva. *ISTEK*. **IX(2)** 18–32.

[12] Hapsari, T.; Tjahjaningsih, W.;, Alamsjah, M. A.; Pramono, A. 2016. Enzymatic Activity of Isolate Proteolytic Bacteria from Gastrointestinal of White Shrimp (Litopenaeus Vannamei). *J Mar Coast Sci*. **5(3)** 109–118.

[13] Walker, J.; Wilson, K. 2005. Protein structure, purification, characterization, and function analysis. In: *Principles and Techniques of Biochemistry and Molecular Biology* 6th ed (Cambridge: Cambridge University Press)

[14] Gunarti, D.R.; Rahmi, H.; Sadikin, M. 2013. Isolation and Purification of Thiamine Binding Protein from Mung Bean. *HAYATI J Biosci*. **20(1)** 1–6.

[15] Robinson, P.K. 2015. Enzymes: principles and biotechnological applications. *Essays Biochem*. **59** 1–41.